

STORM SEVERITY NOWCASTING BY REAL-TIME RETURN PERIOD IMAGING

M. Reyniers¹, L. Delobbe¹, P. Dierickx², M. Thunus², and C. Tricot¹

¹Royal Meteorological Institute of Belgium (RMI)

²Hydrological service of the Walloon administration (Service Public de Wallonie, SPW), Belgium

ABSTRACT

We report on the implementation of a real-time product at the Royal Meteorological Institute of Belgium (RMI) that combines radar data with Intensity-Duration-Frequency (IDF) curves, in order to get an estimate of the return period of an ongoing event, as a measure of the storm severity. The product was developed on request of the hydrological service of the Walloon region (South of Belgium). Experience in this hydrological service has shown that the hydrological model that is used for issuing flood warnings over the Walloon river catchments, performs well in widespread, large-scale precipitation, but that it largely fails in extreme local rainfalls causing flash floods. Therefore, a specialised product allowing fast reaction is needed in these situations. For this purpose, precipitation accumulation images with different durations from two C-band radars are compared in real-time with IDF curves recently determined by the RMI. We will show that, despite the large uncertainties in the rainfall accumulations based on radar data, the product is a very useful nowcasting tool in the case of extreme events.

1 NEED FOR A SPECIALISED PRODUCT

The product is designed to be useful especially in situations with extreme local rainfalls causing flash floods. A stationary precipitating storm cell is a typical example of such a situation. This can happen for example if the cell movement is opposite to the direction of the global flow. Such situations can be dangerous since large amounts of rain are accumulated in the same basin in a short period of time. These situations are, however, hard to recognise on single images, and are only discovered when studying closely the radar animations. An example of such a situation is shown in Fig. 1. We will use this particular situation throughout the paper to illustrate the new product.

2 IDF MAPS AND RADAR DATA

IDF curves (Intensity-Duration-Frequency) give the relation between rainfall intensity I (in mm h^{-1} or mm) in function of the duration (D) of the accumulation and the return period (T). IDF maps for Belgium were recently determined by the RMI (Mohymont & Demarée, 2006). Examples of these maps are given in Fig. 2. The RMI has gauge data of roughly 375 stations. 345 of these station are part of the climatological network, reporting daily accumulation val-

ues. Most of these stations started in 1951. The remaining 30 stations have an update frequency of 10 minutes, and provide data back to 1967. In order to achieve a homogeneous data set to calculate the IDF curves, only those stations were selected with a time series of minimum 25 years, which started before 1968 and ended not sooner than 1993, and in which not more than 10% of the values were missing. With these criteria, the final number of daily stations used in the project decreased to 184, while the 10-min stations decreased to 22. IDF maps were generated by kriging with a resolution of $7 \times 7 \text{ km}^2$.

The storm severity product was implemented for **two radars**. The first one is the weather radar of Wideumont, in the south of Belgium, which is owned and operated by the RMI. It was installed in 2001 and has a maximum range of 240 km. The second one is the radar de l'Avesnois, installed by MétéoFrance in 2005, with a financial participation of the Walloon Region. The maximum range is 256 km. Both radars are C-band radars and generate a pseudo-CAPPI every 5 minutes, which is used here as input for the product. The relation $Z = aR^b$ with $a = 200$ and $b = 1.6$ is applied to convert radar reflectivities into rainrates.

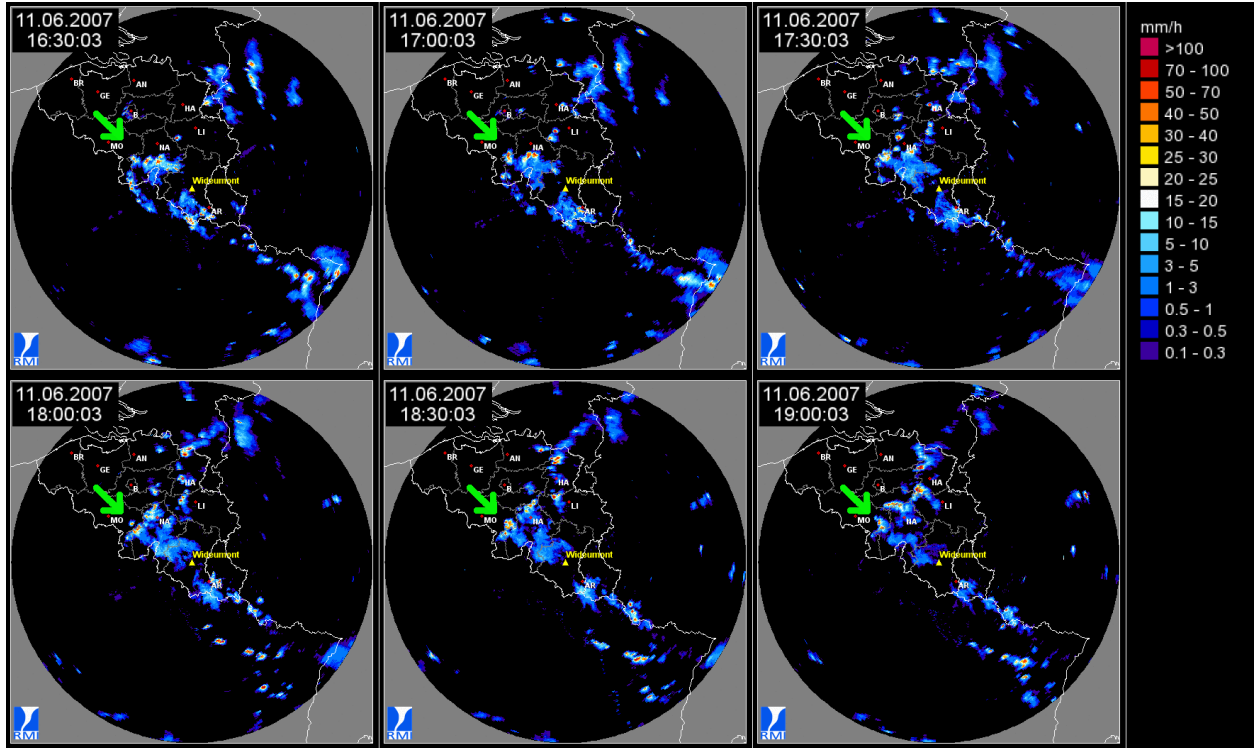


Figure 1: An example of an event with stationary cells (Wideumont radar, 11 June 2007, 16h30-19h00 UT). The green arrow indicates such a cell.

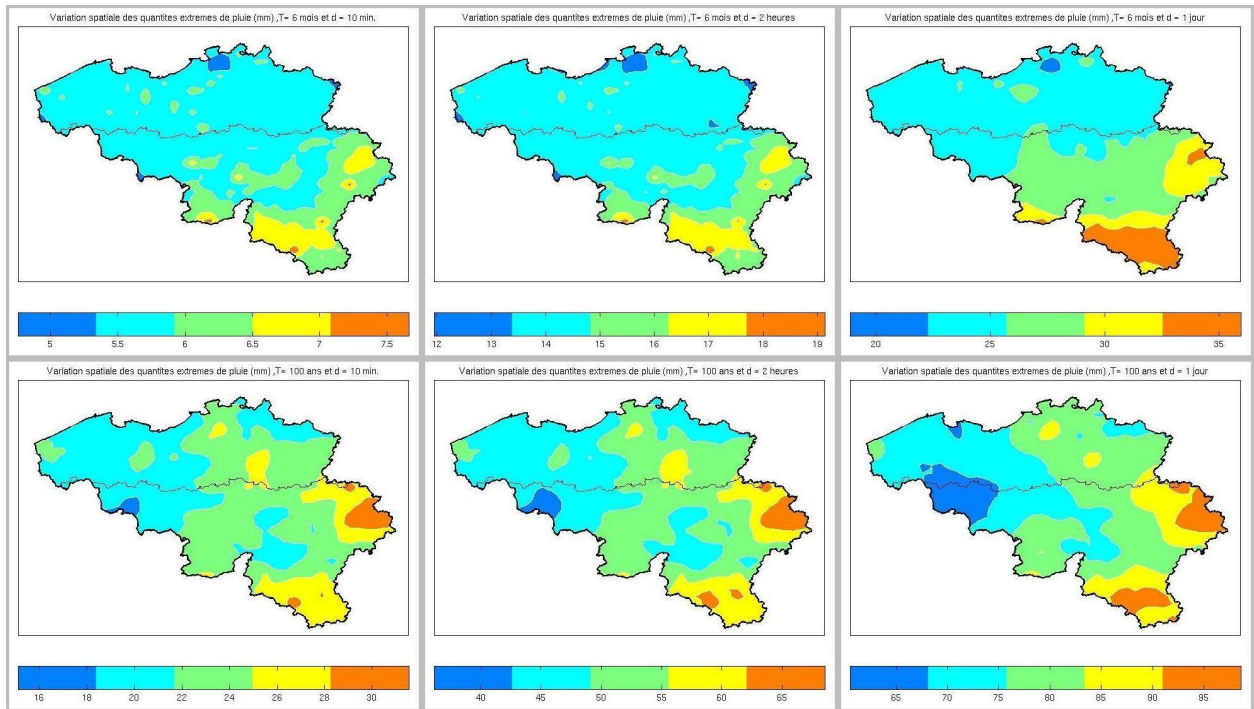


Figure 2: IDF maps (in mm) for a return period of 6 months (upper row) and a return period of 100 years (lower row). For each return period, durations of 10 minutes (left column), 2 hours (middle column) and 1 day (right column) are shown. Note the different scale for each image.

3 METHOD

The preparatory work consisted of the interpolation of the IDF maps to the radar grid of the accumulation images. In the operational context, the following steps are executed every time a new radar image (pseudo-CAPPI) becomes available:

- Calculate the precipitation accumulations for different time windows in a computational cheap way. The accumulations are real-time, so the time windows for these accumulations are “running” (conventional accumulations are calculated for a fixed time span, i.e. between X and Y h UT);
- Combination of the calculated accumulations with the IDF grid to real-time “return-period images”;
- Combination of “return-period images” to one single return-period image as the final output of the product. For every pixel on the map, the maximum of the return periods for that pixel is taken. This maximum is then a measure for the “severity” of the event as it develops.

The method is schematically illustrated in Fig. 3. The real-time accumulations are calculated for the following eight durations: 10 min, 20 min, 30 min, 1 h, 2 h, 6 h, 12 h and 24 h. Every time a new radar image arrives (in normal operation, every five minutes for both radars), each accumulation is updated using this latest image. To minimize the CPU time, the algorithm “recycles” the previous accumulation calculation, and evaluates which radar image has to be added or subtracted from the different accumulation durations. The accumulations of the situation depicted in Fig. 1 are shown in Fig. 4.

4 RESULTS AND DISCUSSION

In Fig. 5 an example of the final product is shown. It is the same case that was shown in Figs. 1 and 4. The map on top shows the maximum return period of the rainfall for the past durations mentioned above, and relies for this on the real-time accumulations discussed in the previous section and calculated following the scheme in Fig. 3. Since the IDF curves were

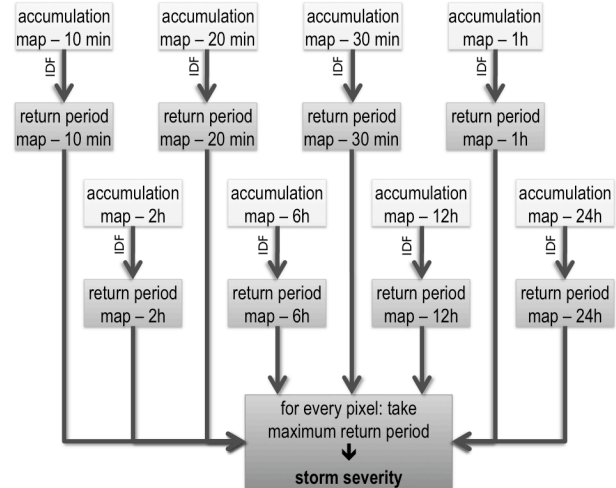


Figure 3: Scheme of the dataflow of the storm severity product.

only calculated for the Belgian territory, the return period map is limited to Belgium as well. The second map (bottom) specifies for which duration this maximum return period is reached, so it expresses at which timescale the most severe rainfall occurred.

From Fig. 5, it is clear that the real-time return period product is a very powerful filter to immediately detect the locations in Belgium that are strongly affected by heavy rain in the past 24h. For example, the region that was marked in Fig. 1 with a green arrow as the location of a stationary cell producing very large local rainfalls, is indeed characterised by a very long return period in Fig. 5.

The real-time return period map can be used to quickly estimate the “severeness” of a given event, without studying loops or browse through the radar archive. However, the end-users should certainly be aware of the limitations of the product. For example, it is well known that for high radar reflectivities, the calculation of a reliable rainrate is hampered by the contamination of hail. In other words: hail produces very high reflectivities, resulting in overestimated rainrates. Therefore the highest return periods (say >30y) are the least reliable, and should only be used qualitatively. In general, the return periods produced by the product should never be used as real and validated climatological values, but only as indicative values.

The accuracy of accumulated rainrates based on radar data, and consequently also of the return pe-

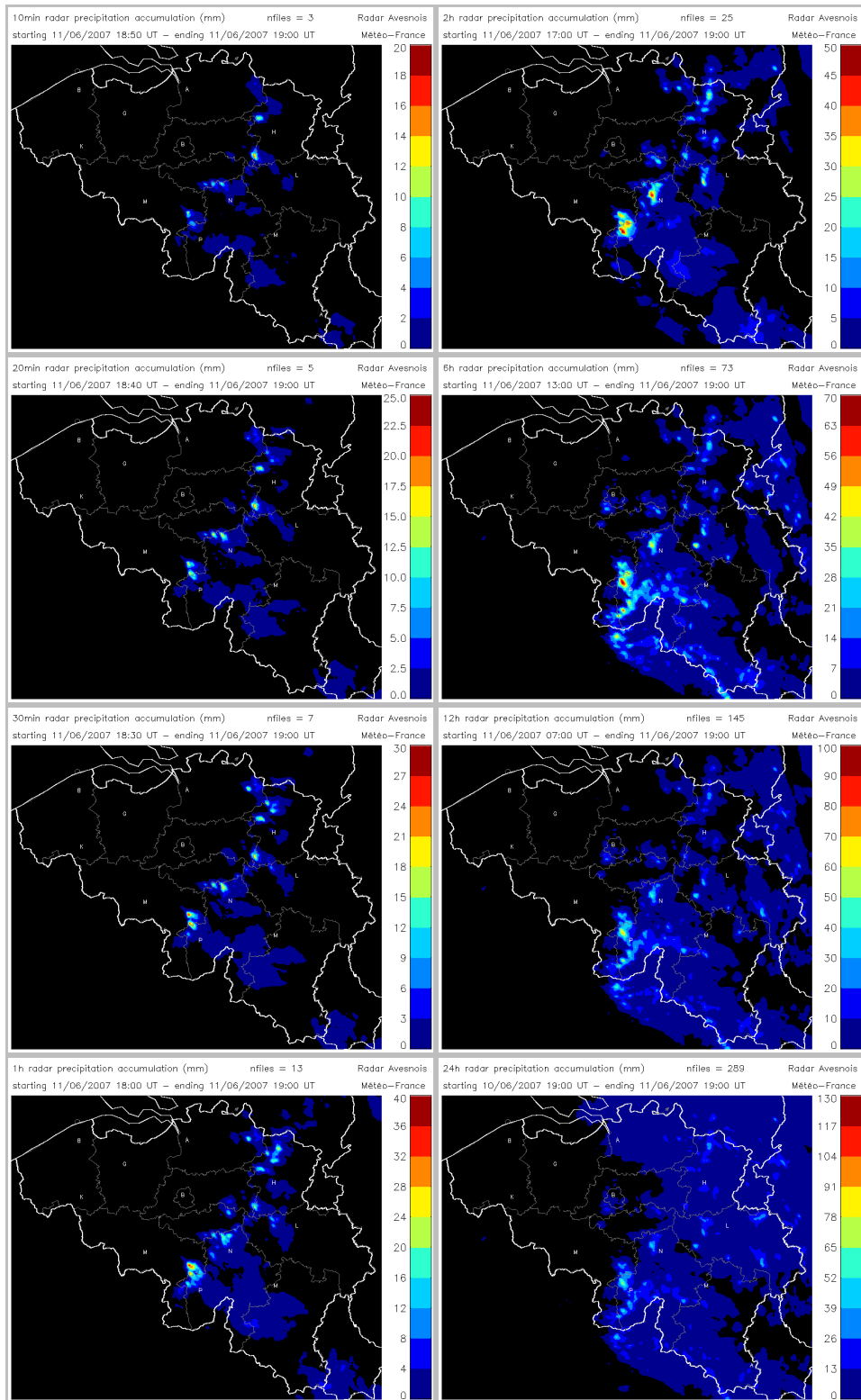


Figure 4: Accumulations for the same situation that was shown in Fig. 1 (radar de l'Avesnois). The following accumulation durations are calculated: *left column* 10 min, 20 min, 30 min, 1 h; *right column* 2 h, 6 h, 12 h and 24 h. The end time of all these accumulations is 19h00 UT. Note that the scale of the images increases for longer accumulation durations.

riods provided by the product, could be significantly improved by correcting the radar images using gauge measurements before ingesting them into the product calculation. Our group (Goudenhoofdt & Delobbe, 2009) recently studied different methods to merge radar data and rain gauges. It turned out that, with relatively simple merging methods, the mean absolute error decreased by 25% with respect to the original data, while more sophisticated methods can achieve a reduction of up to 40%. However, since such kind of product must be available as soon as possible after the receipt of a new radar file, this merging cannot be applied here: the gauges in our network do not have the same update frequency as the radar images. Moreover, the product also focusses on events with very local rainfall; in these situations, the radar-gauge merging is less efficient due to the high spatial variation of the rainfield that cannot be accurately captured by a gauge network, even if it is very dense.

Other notable artefacts that can show up in the final product, are strong contaminations by the bright band, and permanent or anaprop induced ground echoes. These effects are well-known artefacts frequently seen in radar accumulation images, so it is expected that the same effects are seen in the real-time return period images as well. An example of a bright band contamination is shown in Fig. 6. Our group is planning to introduce an operational VPR correction (Vertical Profile of Reflectivity) that should eliminate the bright band effect efficiently. The first results (Mohymont & Delobbe 2008) seem already promising. Note, however, that in Belgium the bright band effect is a typical phenomenon of the cooler seasons, while the product is designed to be used in the case of convective events, that mainly occur in summer.

The final real-time return period map is also quite sensitive to the time sampling of the radar images: if files are missing for a certain period of time, the accumulations, and therefore also the return period map, are rather uncertain. To prevent this, accumulation durations for which more than 10% of the files are missing, are not taken into account in the final return period map.

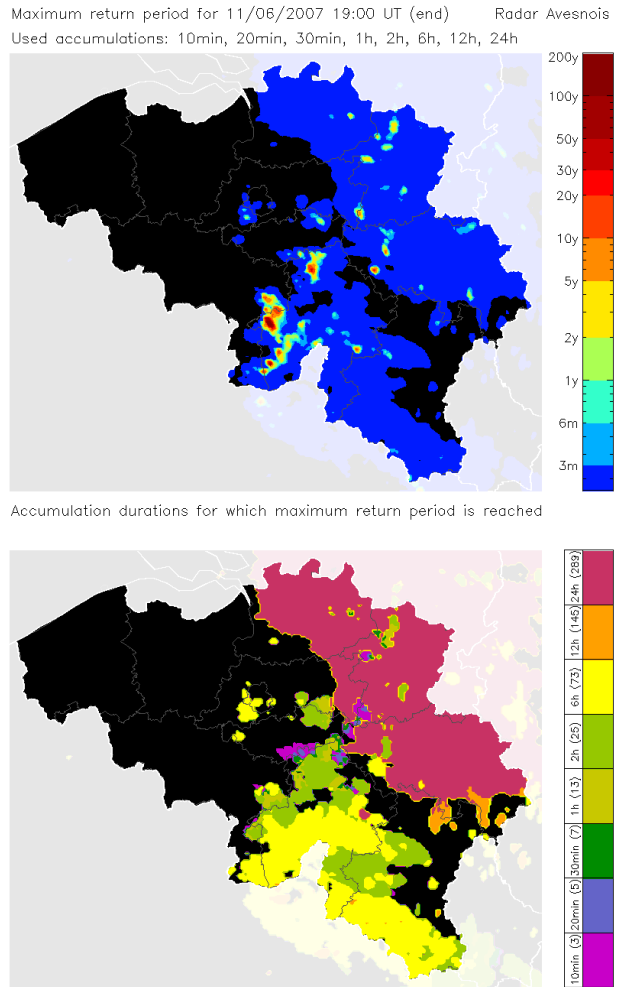


Figure 5: Result of the storm severity product for the same situation that was shown in Fig. 1 (radar de l’Avesnois). The numbers between brackets in the legend of the bottom map denote the number of radar files that were used for that particular accumulation duration.

Maximum return period for 17/04/2009 18:00 UT
Used accumulations: 10min, 20min, 30min, 1h, 2h, 6h, 12h, 24h

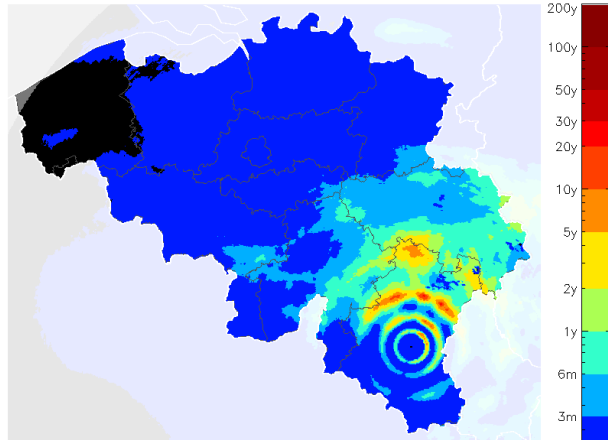


Figure 6: Contamination induced by the bright band for a stratiform situation (Wideumont radar, 17 April 2009, 18h00 UT).

5 CONCLUSION

We have developed a new product at the RMI for the real-time detection of heavy local rainfall. The product will be a valuable nowcasting tool for the real-time evaluation of the severity of an ongoing event, and it will allow fast reaction by the hydrological service in case of potential flash floods, without running a time-consuming hydrological model. However, due to the large uncertainties in radar-based rainfall accumulations and the derived return periods, it offers only a *qualitative* view on the storm severity. This project is part of the new activities of the radar group at the RMI in the framework of nowcasting (see also Goudenhoofdt et al., this volume).

ACKNOWLEDGEMENTS

This research is supported by the Walloon Region (Service Public de Wallonie). We are indebted to MétéoFrance for providing us the radar data of l'Avesnois. Christophe Ferauge and Geert De Sadelaer are thanked for the technical support in the development.

REFERENCES

Goudenhoofdt E., Delobbe L., 2009, "Evaluation of radar-gauge merging methods for quantitative precipitation estimates", *Hydrology and Earth System Sciences*, 13, 195–203

Mohymont B. and Demarée G.R., 2006, final report IDF curves for the Walloon region, Ministère Wallon de l'Équipement et des Transports, Cahier spécial des charges MS/212/2003/08, available on <http://voies-hydrauliques.wallonie.be/>

Mohymont B. and Delobbe L., 2008, "Analysis of the mean and the variability of the vertical profile of reflectivity over Belgium", proceedings of ERAD2008, the Fifth European Conference on Radar in Meteorology and Hydrology, Helsinki, Finland, June 30 - July 4, 2008